ORIGINAL ARTICLE

Modification of 3D Printed Polylactic Acid Scaffold with Chitosan and Polyvinyl Alcohol in Enhancing Bone Mineralization

Ravathi Marathandi [1], Hemalatha Mariapen[1], Murfiqah Taufiqiah Mohd Amin[1], Norhana Jusoh[1,2,3]

[1] Department of Biomedical Engineering and Health Sciences, Faculty of Electrical Engineering, Universiti Teknologi Malaysia, 81310 UTM Johor Bahru, Johor, Malaysia

[2] Medical Device Technology Center (MEDiTEC), Institute Human Centred Engineering (iHumEn), Universiti Teknologi Malaysia, 81310 UTM Johor Bahru, Johor, Malaysia

[3] Bionspired Device and Tissue Engineering Research Group, Department of Biomedical Engineering and Health Sciences, Universiti Teknologi Malysia, Faculty of Electrical Engineering 81310 UTM Johor Bahru, Johor, Malaysia

ABSTRACT

Introduction: Bone tissue engineering (BTE) with three-dimensional (3D) scaffolds has been developed to create complex and tissue-specific structures for regeneration. In this study, polylactic acid (PLA), a common polymer in 3D printing, was utilized despite its limitations in bioactivity, biomineralization, and hydrophilicity. Polyvinyl alcohol (PVA) and chitosan (CS) that known for their excellent biological properties were used for surface modification of the 3D-printed PLA properties. **Methods:** PLA scaffolds were fabricated via 3D printing and subsequently coated with PVA and CS using a combination of dip coating and freeze-drying techniques. The coated scaffolds were characterized using scanning electron microscopy (SEM), Fourier Transform Infrared Spectroscopy (FTIR), Energy Dispersive X-ray (EDX), and water contact angle (WCA) measurements. **Results:** PLA/CS/PVA scaffolds exhibited the highest hydrophilicity, with a WCA of 48.43 ± 5.55°. SEM analysis revealed a smooth and continuous PVA film, alongside irregular CS patches. FTIR confirmed the successful chemical bonding of PLA, CS, and PVA. EDX analysis detected calcium (Ca) and phosphate (P) ions, with a Ca/P ratio of 2.76, closely resembling human bone, as compared to a ratio of 2.07 in pure PLA scaffolds. **Conclusion:** The 3D-printed PLA scaffold with dual PVA/CS coatings demonstrated good biomineralization that advantage for bone regeneration applications.
Malaysian Journal of Medicine and Health Sciences (2025) 21(SUPP11): 15-23.doi:10.47836/mjmhs.21.s11.3

Keywords: 3D Printing, Chitosan, Polylactic acid, Polyvinyl alcohol, Bone mineralization.

Corresponding Author:
Norhana Jusoh, PhD
Email : norhana@utm.my
Tel : +60122535206

INTRODUCTION

Bone primarily function is to provide structural support for tissue and the body. Bone tissue provides mineral homeostasis that supplies calcium phosphate, magnesium, potassium, and bicarbonate to mobilize the mineral reservoir [1]. Bone is a dynamic tissue that can be rebuilt by remodeling to maintain its function capability, which has the ability of self-renewal and regeneration when damaged or injured. Prolonged life expectancy and the growth of an aging population contribute to conditions like degenerative bone diseases that made bone as the second most transplanted tissue in the world [2]. Bone grafting promotes bone healing through osteoconduction, osteogenesis, and osteoinduction; however, it has limitations, including limited donor availability, risk of infection, donor site morbidity, and high risks due to the surgical interventions required. Therefore, bone tissue engineering (BTE) is an evolving technique to reduce the limitations of bone grafts and provide a solution for using scaffolds to regenerate bone tissues.

An ideal scaffold is designed and constructed for cell adhesion, proliferation, and differentiation by mimicking extracellular matrix (ECM) in the human body, such as ECM bone tissue. To obtain the final biological response, it is required to design an ideal three-dimensional design by controlling nano to microstructures [3]. The scaffold is important for providing regenerative signals to the cells and stimulating natural behaviors.

The fabrication methods of bone scaffolds are also an important consideration. The conventional method such as gas foaming, freeze drying, and particulate leaching method is a technique that allows for porous matrices and relatively easy processability. However, the conventional methods have limitations such as poor reproducibility, uncontrolled pore shapes, size, and geometry, and limited interconnectivity of scaffold design [4]. The recent development of three-dimensional (3D) printing has improved the design and repeatability of the scaffold as it provides control over spatial geometry, scaffold design and productivity between prints [3]. Three-dimensional printing also known as additive manufacturing (AM), is the most effective and developing technology in bone tissue engineering due to its capability in fabricating different types of materials with customized shapes and dense or macro/micro porous scaffold architecture. Fused deposition modelling (FDM) is the main type 3D printing technology that have been utilize in developing bone scaffolds due to its simplicity and relatively reproducible method that support the reconstruction of tissue with the active substances such as cells and growth factors that eventually offer good biocompatibility, osteoinductive and biodegradability properties [5].

Polylactic acid (PLA) is a polymer biomaterial which is a highly biocompatible and renewable source derived through the fermentation of sugars [6]. Besides, PLA has good thermal properties, degradation resistance, low viscosity and thermoplastic properties which suitable for FDM technology. However, pure PLA scaffolds have limited bioactivity and poor hydrophilicity, which hinders their ability to support effective biomineralization and integration in biological environments. Hydrophobicity of PLA material contribute to poor cell adhesion and protein activation and signaling. These limitations are due to PLA's lack of functional groups that facilitate interactions with biominerals and water, leading to minimal and uneven mineral deposition and low water uptake [7]. The chiral molecule of PLA consists of two enantiomers, l- and d- lactic acid, such as poly(l-lactide) (PLLA) and poly(d-lactide) (PDLA), which slows down the surface wettability and bioactivity [6].

Even though the ideal scaffold structure is to allow cell attachment, proliferation, adhesion, and differentiation, cell interfaces is limited on this PLA material. Therefore, surface modification techniques may overcome the limitations of pure PLA. Exploring a simple, effective surface modification technique for PLA scaffolds is important for understanding the suitable incorporation of biomaterials in scaffolds. Previously, PLA scaffolds have been coated with bioactive materials such as chitosan (CS) and hyaluronic acid/polyvinyl alcohol (PVA) in enhancing the scaffold properties [8,9]. As a natural polymer, CS is known for its excellent biocompatibility and bioactivity, promoting better interaction with minerals. Chitosan has biological properties, including antimicrobial activity and the ability to support ECM mineralization, as the amino groups in CS can attract calcium ions, facilitating the deposition of calcium phosphate minerals essential for bone regeneration [10, 11]. Therefore, coating PLA scaffolds with CS creates a bioactive surface that promotes biomineralization.

Similarly, PVA has advantages in enhancing hydrophilicity, primarily due to its chemical structure. PVA is a synthetic polymer characterized by the presence of hydroxyl groups (-OH) along its backbone [12]. These hydroxyl groups have a strong affinity for water molecules, making PVA highly water-soluble and hydrophilic [12]. Although PVA itself is not bioactive, it provides an excellent matrix for incorporating bioactive substances, such as hydroxyapatite or other calcium phosphates.

The combination of CS and PVA's coating on PLA scaffolds aims to synergistically improve both bioactivity and hydrophilicity, thereby enhancing biomineralization and creating a more suitable environment for tissue integration. According to recent reviews on PLA scaffold surface modifications, only few studies have examined the effects of PVA or dual PVA/CS coatings, and none have specifically focused on their application to 3D-printed PLA scaffolds [4]. Therefore, this research aims to provide new insights of the effect of CS and PVA dual coating on the surface modifications, biomineralization, and wettability of 3D-printed PLA scaffolds.

MATERIALS AND METHODS

Materials

Polylactic acid filament (1.75mm) purchased from FLASHFORGE Corp. (China), PVA powder, CS powder, deionized water, and acetic acid for dip coating the PLA scaffold into the prepared solution. Sodium hydroxide (NaOH), sodium bicarbonate (NaHCO3), potassium chloride (KCl), potassium phosphate (K_2HPO_4), magnesium chloride ($MgCl_2$), calcium chloride ($CaCl_2$), sodium sulfate (Na_2SO_4), tris(hydroxymethyl) aminomethane ($(CH_2OH)_3CNH_2$), and 1M hydrochloric acid (HCl) are the nine chemicals used to prepare simulated body fluid (SBF) solution, which mimics human blood plasma.

Fabrication of 3D Printed PLA Scaffold

SolidWorks software was used to design scaffolds, which were saved in Standard Triangulate Language (.stl) files compatible with the printer software. A specific 0.4mm diameter nozzle (Creator Pro 2, Flashforge, China) and FlashPrint 5 software were employed for fabricating the PLA scaffold using the FDM method. The STL files were imported into the slicer software to generate G-codes, which were then transferred to the 3D printer. PLA filament with a diameter of 1.75mm was used as the printing material. During printing, the 3D printer

heated the PLA filament, and the scaffold was printed layer by layer to achieve controlled pore dimensions. The designed scaffold was cubic, measuring 9.9mm x 9.9mm, with struts that were 0.9mm thick and consistent square pores with a diameter of 0.9mm. Men et al. (2024) mentioned, based on a simulation, that scaffolds with 900μm pores are more advantageous to bone tissue growth [13]. Each scaffold took approximately 18 minutes to complete printing.

Coating of 3D Printed PLA Scaffold with PVA and CS

The PLA scaffolds were soaked in distilled water for 1 hour prior ultrasonication for 5 minutes. The scaffolds underwent hydrolysis with a 0.1 M NaOH solution at 65°C for 45 minutes with constant agitation. Then, the scaffolds were washed three times with deionized water to remove NaOH residues in enhancing surface roughness and increasing coating adhesion [14]. The coating solutions were prepared by dissolving CS at 2 wt% in 2 wt% acetic acid and PVA at 4 wt% in distilled water at 80°C [15]. After 24 hours, the solutions were filtered and mixed with equimolar blend of CS: PVA at a ratio of 50:50 mol% [15]. The mixture was stirred for another 24 hours to ensure homogeneity. Next, dip coating was done by immersing the 3D printed PLA scaffold for 5 minutes each in CS, PVA, and PVA/CS solutions [16]. The dip-coated samples were frozen in the freezer for more than 24 hours [17] and then subjected to freeze-drying to preserve their biological and chemical structures through sublimation.

SBF Solution Preparation

Preparation of the SBF solution was done based on Kokubo's method with the composition and pH mimicking human blood plasma conditions [18]. All glassware and containers were cleaned by using 1M HCl solution as the neutral detergent and ion-exchanged distilled water, followed by drying process. In a one-liter polyethylene bottle containing 500 ml of ion-exchanged distilled water, all reagents were sequentially dissolved to achieve the SBF composition [18]. The solution temperature was carefully regulated at 36.5°C by using a water bath. The pH adjustment to 7.40 was achieved through titration with a 1N HCl solution. After transferring the solution to a volumetric flask and adjusting the volume to one liter with ion-exchanged distilled water at 20°C, the SBF solution was stored in a refrigerator at 5–10°C in a suitable container for later use.

Scanning Electron Microscope (SEM) and Energy-Dispersive X-ray Spectroscopy (EDX) Analysis

The surface morphology of 3D-printed PLA scaffolds coated with PVA and PVA/CS was evaluated by using a scanning electron microscope (SEM, Hitachi TM3000 Tabletop, Japan) equipped with an energy-dispersive X-ray spectroscopy (EDX) system. The scaffold surfaces were sputter-coated with gold before analysis to enhance the conductivity. Morphology observations were made before and after SBF testing at magnifications of 50x and 80x with 5kV, and at 1000x with 15kV. The EDX analysis was conducted with an accelerating voltage of 5kV and a dwell time of approximately 15 seconds, displayed the elemental composition in weight percent (wt.%) following SBF testing, providing insights into the scaffolds' bioactivity and mineralization.

Water Contact Angle (WCA) Analysis

The surface wettability of the scaffolds was analyzed by using a contact angle goniometer (VCA optima XE, AST Product Inc., USA). Distilled water was first loaded into a syringe and using the static mode of the sessile drop method, a 4 μl droplet of distilled water was deposited on the sample surface.

Fourier-Transform Infrared Spectroscopy (FTIR) Analysis

Fourier-transform infrared spectroscopy (FTIR, PerkinElmer Inc., USA) was conducted to analyze the chemical structures and surface functional groups of 3D-Printed PLA, PLA/CS, PLA/PVA, and PLA/CS/PVA scaffolds. The samples were prepared and positioned in the FTIR spectrometer, with the analysis carried out in the mid-infrared range (4000 $cm^{-º}$ to 400 $cm^{-º}$) at a resolution of 4 $cm^{-º}$ to ensure clear spectral details. The data was further processed using OriginPro software (OriginLab, USA) to identify specific peaks in the spectrum.

Biomineralization Testing

The 3D-printed PLA, PLA/CS, PLA/PVA, and PLA/PVA/CS scaffolds were immersed individually in SBF solution maintained at a constant temperature of 36.5°C. The SBF was exchanged weekly, and just before replacement, the calcium ion concentration and pH were measured [19]. After immersion periods of 7, 14, and 21 days, the specimens were extracted from the SBF, rinsed thoroughly with deionized water multiple times, and subsequently dried at ambient temperature for two days [19]. The formation of an appetite layer on the surface of the scaffolds was investigated to evaluate surface properties using SEM and EDX analysis.

RESULTS

Fabrication of 3D Printed PLA Scaffolds

The scaffold was designed to be cubic, with dimensions of 9.9 mm (length), 9.9 mm (height), and 9.9 mm (width), that preferably have high compressive strength. The square pores measuring 0.9 mm and struts with a diameter of 0.9 mm, were arranged in layers to mimic the microenvironment of the native ECM. This design facilitates the transportation of nutrients, waste products, and the supply of oxygen [20]. Fig 1 illustrates the complete architecture of the scaffold design and the results after 3D printing fabrication.

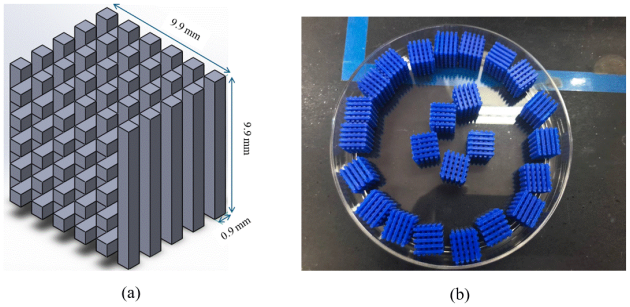

Fig 1 : Image of (a) CAD design and (b) 3D printed of PLA scaffold.

Surface Morphology

The SEM analysis was conducted to observe the surface morphology of PLA, PLA/CS, PLA/PVA, and PLA/PVA/CS scaffolds, as shown in Fig. 2. At low magnifications (x50 and x80), the SEM images of pure PLA scaffolds exhibit a smooth and even surface with aligned and uniform layers, attributed to the 3D printing process [17]. Minor imperfections and pores were visible on the surface due to the extrusion method used in printing. Additionally, the PLA's tendency to absorb moisture from the air makes it brittle and susceptible to breakage, leading to print quality issues like steam bubbles and extruder blockages, as well as filament swelling [21]. The uncoated PLA scaffold used as a control for comparing the effects of subsequent coatings.

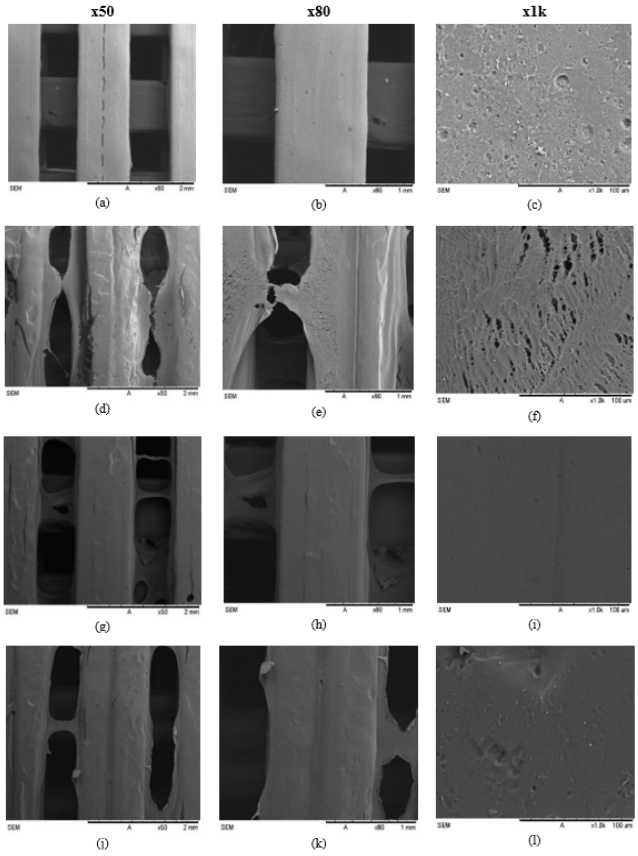

Fig 2 : SEM images of 3D printed scaffold at different magnifications (x50, x80, x1000) for (a-c) PLA, (d-f) PLA/CS, (g-i) PLA/PVA and (j-l) PLA/CS/PVA.

The SEM images showed that coating with CS produced a thin film over the PLA scaffold, partially filling surface pores and creating a granular texture. At higher magnification, small CS particles were visible, which increased surface roughness. In contrast, PVA coating generated a smooth and uniform film that covered the surface and reduced irregularities. When both polymers were combined, the PLA/CS/PVA scaffolds displayed features of both coatings like a continuous smooth film from PVA with occasional rough patches from CS. This dual effect improved surface uniformity while retaining added roughness, which may enhance coating stability and cell interactions.

Surface Wettability Analysis

The water contact angle of the PLA, PLA/CS, PLA/PVA, and PLA/PVA/CS scaffolds was measured using a goniometer to determine surface wettability. Water droplets were placed on different locations on each scaffold's surface, and measurements were taken five times to obtain average values with standard deviation, as summarized in Table I. The mean contact angle for pure PLA was recorded at 111.90° ± 1.83°, indicating its hydrophobic nature. This high contact angle reflects PLA's poor interaction with water, which can limit its bioactivity and performance in applications requiring good moisture interaction [22].

With the addition of a CS coating, the scaffold's wettability was improved. As a hydrophilic material, CS reduced the contact angle and enhanced PLA's surface interaction with water. The PLA scaffold coated with PVA showed an even more significant reduction in contact angle, recording a mean value of 70.10° ± 2.03°, indicating that PVA's highly hydrophilic nature makes the surface considerably more water-interactive. The dual coating of PVA and CS on PLA resulted in the most significant improvement in wettability, with a mean contact angle of 42.80° ± 5.55°. This substantial decrease in contact angle indicates a highly hydrophilic surface, ideal for efficient water interaction.

Table I: Surface wettability readings of samples.

Sample	Average value of WCA
PLA	111.90 ± 1.83
PLA/CS	82.73 ± 1.60
PLA/PVA	71.90 ± 2.03
PLA/CS/PVA	48.43 ± 5.55

FTIR Analysis

The FTIR spectrum in Fig 3 shows the peaks and chemical bonding of PLA, PLA/CS, PLA/PVA, and PLA/CS/PVA scaffolds. The FTIR spectra of various PLA-based scaffolds revealed their chemical structure and interactions. Pure PLA showed characteristic peaks at 3330 cm^{-o} (O-H stretching), 2956 cm^{-o} (C-H stretching), and 1736 cm^{-o} (C=O stretching). The PLA/CS scaffold

demonstrated the integration of chitosan, shown by a broad peak around 3355 cm^{-o} (N-H stretching) and the amide I band at 1633 cm^{-o}, while retaining PLA's structural features [24]. In the PLA/PVA scaffold, strong hydrogen bonding is evidenced by a broad O-H stretching peak at 3274 cm^{-o}, with additional peaks at 1742 cm^{-o} (C=O stretching) and 1328 cm^{-o}. The PLA/PVA/CS composite shows peaks at 3288 cm^{-o} (O-H stretching), 1736 cm^{-o} (C=O stretching), and interaction peaks at 1528 cm^{-o} and 1326 cm^{-o}, which are absent in pure PLA [8]. These results confirm the successful incorporation of CS and PVA into the PLA scaffold, enhancing its properties through distinct chemical interactions.

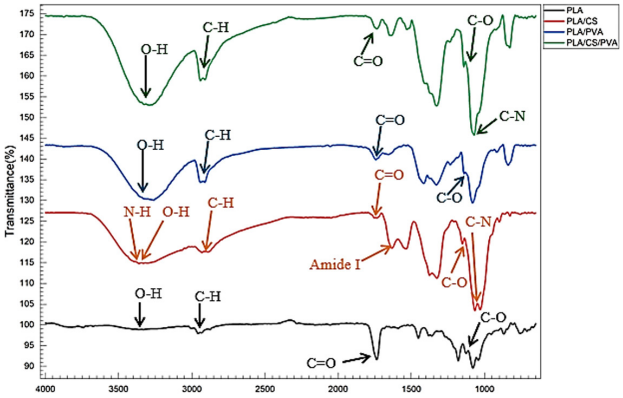

Fig 3 : FTIR spectrum of PLA, PLA/CS, PLA/PVA, PLA/CS/PVA.

Biomineralization

Biomineralization testing of the PLA, PLA/CS, PLA/PVA, and PLA/CS/PVA scaffolds using SBF was verified through SEM and EDX analyses. Fig 4 displays the SEM images, illustrating mineral layer formation on each scaffold's surface, while EDX analysis provides the elemental composition data for these samples. SEM analysis shows that pure PLA exhibits a smooth surface with minimal mineral deposits, reflecting limited bioactivity due to its lack of functional groups that interact with calcium and phosphate ions. In contrast, PLA scaffolds coated CS displayed substantial changes after immersion in SBF, with a rougher surface and a dense network of mineral particles, attributed to CS's amino and hydroxyl groups that promote mineral growth [23]. Besides that, PLA coated with PVA also shows mineral deposition, though it appears less uniform and continuous compared to the CS-coated scaffold. The dual coating of CS and PVA on PLA results in a densely mineralized surface with a thick layer of apatite-like minerals, indicating a strong enhancement in biomineralization.

Based on table II of the EDX analysis supports these observations, showing changes in elemental composition after coating. Oxygen (O) remains the main element, maintaining scaffold integrity, while sodium (Na) and magnesium (Mg) levels increase in the PLA/CS/PVA scaffold, indicating improved water affinity and bioactivity. Phosphorus (P) levels are higher in the coated scaffolds, further suggesting enhanced bioactivity, while the increased calcium (Ca) concentration in PLA/CS/PVA scaffolds points to a better biomineralization ability [24].

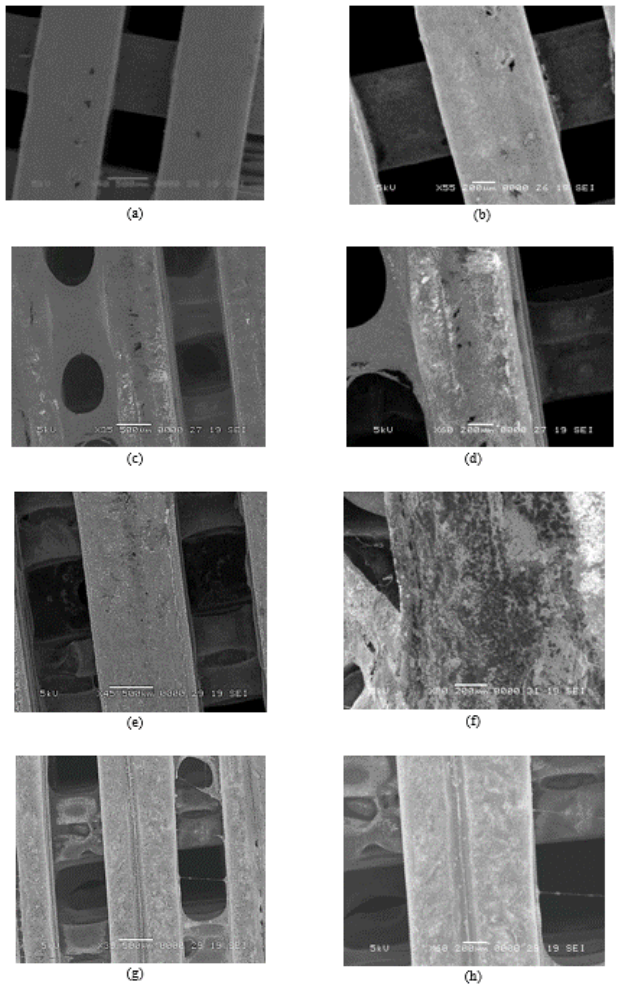

Fig 4 : SEM image of mineralization testing at different magnifications for (a-b) PLA, (c-d) PLA/CS, (e-f) PLA/PVA and (g-h) PLA/CS/PVA scaffold

Table II : Weight percentage of elements in samples.

Elements	Weight (%) of samples			
	PLA	PLA/CS	PLA/PVA	PLA/CS/VA
Oxygen	33.419	39.453	35.808	39.286
Sodium	18.457	21.913	19.078	30.073
Magnesium	0.850	1.448	0.950	5.902
Phosphorus	3.934	6.890	4.380	8.510
Chlorine	36.508	42.407	36.897	38.163
Calcium	8.135	17.790	11.075	22.502

The Ca/P ratios of the scaffolds are summarized in Table III. The PLA/CS/PVA coated scaffold has the highest Ca/P ratio of 2.76, suggesting enhanced biomineralization and the ability to form hydroxyapatite (HA), which is essential for bone growth and regeneration. PLA/CS has a Ca/P ratio of 2.58, showing good mineral activity, while PLA/PVA follows with a ratio of 2.53. Pure PLA, with the lowest ratio at 2.07, exhibits reduced mineralization potential.

Table III : Atomic content of Ca and P in samples

Elements	PLA		PLA/CS		PLA/PVA		PLA/CS/PVA	
	Atomic (%)	Ca/P	Atomic (%)	Ca/P	Atomic (%)	Ca/P	Atomic (%)	Ca/P
Ca	8.135	2.07	17.790	2.58	11.075	2.53	23.502	2.76
P	3.934		6.890		4.380		8.510	

DISCUSSION

The SEM analysis highlights the impact of CS and PVA coatings on PLA scaffold surface morphology. The smooth and even surface was observed on the uncoated PLA scaffold with minor flaws due to printing process. This type of scaffold was prone to brittleness and extruder blockages due to PLA's moisture-absorbing properties [21]. Adding a CS coating creates a thin layer that fills some pores and introduces a granular surface texture. The CS particles was observed at higher magnification which suggest improved surface roughness that potentially enhanced cell attachment properties. In comparison, the PVA-coated PLA scaffold displays a smoother, more continuous film, reducing surface irregularities and indicating enhanced scaffold uniformity. The combined PVA/CS coating allows the scaffold surface to retain PVA's smooth, uniform film while introducing localized roughness from CS. This balance between uniform coverage and added roughness enhances hydrophilicity, improves coating stability, and provides favorable sites for cell attachment and mineral deposition in bone [25]. Similar synergistic effects of combining polymers such as PVA and CS on surface morphology and bioactivity have also been reported [26].

The wettability analysis highlights the impact of various coatings on the surface properties of PLA scaffolds. The hydrophobic nature of pure PLA, indicated by its high contact angle, limits its suitability for applications that require efficient water interaction. The application of CS coating improves PLA's wettability due to CS's hydrophilic properties, making the scaffold more conducive to water interaction and potentially enhancing its bioactivity. A further improvement was observed with PVA coating, which significantly lowers the contact angle, suggesting an increased in surface hydrophilicity. The coating of PVA and CS produced the most hydrophilic surface, which is favorable for cell adhesion and growth [27]. This is because PVA increases wettability, while CS provides amino and hydroxyl groups that promote protein binding, creating a surface suitable for protein adsorption, cell attachment, and bone tissue formation. Cells generally attach better to hydrophilic surfaces, and human fetal osteoblastic cells (hFOB) have been reported to prefer surfaces with a water contact angle below 60° [28] This enhanced hydrophilicity from the dual coating offers substantial bioactivity advantages, making it suitable for applications in tissue engineering.

The FTIR spectra analysis reveals characteristic peaks for each scaffold, highlighting the successful incorporation and interaction of CS and PVA into the PLA matrix. Pure PLA displays typical peaks for C=O and C-H stretching, with an O-H stretching peak suggesting possible moisture absorption [29]. The PLA/PVA/CS scaffold integrates the features of all three components, confirmed by strong hydrogen bonding and intermolecular forces, creating a composite material with enhanced structural properties and bioactivity potential [8,24]. In addition, NaOH hydrolysis pretreatment introduced carboxyl groups, promoting mechanical interlocking of the coating within the surface irregularities. The observed shifts in O-H, N-H and C=O from the interaction peaks at 1528 cm^{-o} and 1326 cm^{-o} highlight the formation of new hydrogen bonding and electrostatic adsorption between PLA, PVA, and CS. This suggests that the coating adhered to both mechanical interlocking with physicochemical interactions with previous reports on scaffold coatings [30-32]. These findings confirm the successful incorporation of CS and PVA, which enhances the scaffold's surface characteristics and coating adherence, through both mechanical interlocking and adsorption. In addition, it also enhances hydrophilicity and improves mineralization as reported by EDX findings.

The biomineralization testing results show significant variations in surface morphology and mineral deposition among the different scaffold coatings. Pure PLA exhibited minimal mineral deposition and limited bioactivity, attributed to its lack of functional groups that can effectively interact with calcium and phosphate ions. The addition of CS coating to PLA greatly enhances mineral deposition, with SEM images displaying a rough surface and dense mineral network. This improvement might be due to CS's amino and hydroxyl groups, which facilitate mineral growth, thus increasing biomineralization of scaffolds [11].

The PLA coated with PVA also shows increased mineralization compared to pure PLA, but its deposition pattern appears less uniform than that seen in the PLA/

CS scaffold. However, the dual CS and PVA coating on PLA exhibits the most substantial improvement, resulting in a thick layer of apatite-like minerals that indicate enhanced mineralization analysis confirms the impact of these coatings on elemental composition. Increased in Na and Mg levels in PLA/CS/PVA scaffolds suggest improved water affinity, while higher P and Ca concentrations demonstrate enhanced bioactivity.

The PLA/CS/PVA scaffold showed the highest Ca/P ratio (2.76), which indicates a calcium-rich mineral phase. However, a higher Ca/P ratio is not always better for biomineralization because stoichiometric hydroxyapatite (HA) has a Ca/P ratio of 1.67, and large deviations from this value may form non-stoichiometric or unstable phases [33-34]. Therefore, the mineralization quality should be discussed using both elemental ratios and surface morphology. In this study, the PLA/CS/PVA scaffold showed higher Ca and P levels together with a dense mineral layer in SEM images, which suggests improved mineralization even though the Ca/P ratio was higher than 1.67.

CONCLUSION

The development of 3D-printed PLA scaffolds coated with PVA and CS were successfully demonstrated with improved hydrophilicity and bioactivity properties. The fabricated scaffolds were analyzed in terms of surface and chemical properties, including surface morphology, chemical composition, and wettability. The addition of CS introduced a granular texture, while the PVA coating created a smoother and more uniform surface. Thus, the 3D printed PLA/CS/PVA scaffold have both features that enhancing its surface characteristics. The surface wettability analysis showed that the dual-coated scaffold had the highest wettability. Biomineralization testing confirmed the presence of calcium and phosphate ions, essential for bone formation, on the scaffold surfaces. According to the SEM results, all the scaffolds achieved good porosity and interconnectivity, which are ideal properties for bone scaffolds. Moreover, EDX and FTIR analyses confirmed the presence of the desired elements in the scaffold. The results demonstrated that 3D-printed PLA coated with PVA and CS has great potential for bone scaffolds. The findings suggest that PVA and CS coatings improved the surface morphology, chemical functionality, wettability, and biomineralization capabilities of the PLA scaffold. These enhancements suggest that the modified 3D-printed scaffolds could provide better performance in BTE applications by offering improved functionality, which are critical for effective bone regeneration in critical-size defects.

ACKNOWLEDGEMENT

This work was supported by RUG-UTM Matching Grant (Q.J130000.3023.04M47) from Universiti Teknologi Malaysia, Malaysia.

REFERENCES

1. Manzini BM, Machado LMR, Noritomi PY, Da Silva J V.L. Advances in Bone tissue engineering: A fundamental review. Journal of Biosciences. 2021;46(1);17. doi.org/10.1007/s12038-020-00122-6
2. Lee SS, Du X, Kim I, Ferguson SJ. Scaffolds for bone-tissue engineering. Matter. 2022;5(9): 2722–2759. doi.org/10.1016/j.matt.2022.06.003
3. Wang C, Huang W, Zhou Y, He L, He Z, Chen Z, et al. 3D printing of bone tissue engineering scaffolds. Bioactive Materials. 2020;5(1):82–91. doi.org/10.1016/j.bioactmat.2020.01.004
4. Collins MN, Ren G, Young K, Pina S, Reis RL, Oliveira JM. Scaffold Fabrication Technologies and Structure/Function Properties in Bone Tissue Engineering. Advanced Functional Materials. 2021;31(21):2010609. doi.org/10.1002/adfm.202010609
5. Zhang Q, Zhou J, Zhi P, Liu L, Liu C, Fang A et al. 3D printing method for bone tissue engineering scaffold. Medicine in Novel Technology and Devices. 2023;17:100205. doi.org/10.1016/j.medntd.2022.100205
6. Kačarević ŽP, Rider P, Alkildani S, Retnasingh S, Pejakić M, Schnettler R. An introduction to bone tissue engineering. The International Journal of Artificial Organs. 2019;43(2), 69–86. doi.org/10.1177/0391398819876286
7. Castaceda-Rodrнguez S, González-Torres M, Ribas-Aparicio RM, Del Prado Audelo ML, Leyva Gymez G, Gürer, E. S. Recent advances in modified poly (lactic acid) as tissue engineering materials. Journal of Biological Engineering. 2023;17(1). doi.org/10.1186/s13036-023-00338-8
8. Farsi M, Asefnejad A, Baharifar H. A hyaluronic acid/PVA electrospun coating on 3D printed PLA scaffold for orthopedic application. Progress in Biomaterial 2022;11(1):67–77. doi.org/10.1007/s40204-022-00180-z
9. Goswami K, Garg M, Sharma P, Negi A, Bhardwaj D, Kanwar M, et al. 3D Printed PLA Scaffolds Modified with Chitosan-Based Electrospun Nanofibers for Biomimetic Mineralization and Antimicrobial Efficacy. Journal of Applied Polymer Science, e58022. doi.org/10.1002/app.58022
10. Tian Y, Wu D, Wu D, Cui Y, Ren G, Wang Y, et al. Chitosan-based biomaterial scaffolds for the repair of infected bone defects. Frontiers in Bioengineering and Biotechnology. 2022;10:899760. doi.org/10.3389/fbioe.2022.899760
11. Hu D, Ren Q, Li Z, Zhang L. Chitosan-based biomimetically mineralized composite materials in human hard tissue repair. Molecules. 2020;25(20):4785. doi.org/10.3390/molecules25204785
12. Nagarkar R, Patel J. Polyvinyl alcohol: a comprehensive study. Acta Sci. Pharm. Sci.2019;

3(4), 34-44.
13. Men Y, Wei L, Hu B, Hao P, Zhang, C. Simulation research on the influence of regular porous lattice scaffolds on bone growth. PubMed, 2024;42(4),808–816. doi.org/10.7507/1001-5515.202410062
14. Schneider M, Fritzsche N, Puciul-Malinowska A, Baliś A, Mostafa A, Bald I. Surface Etching of 3D Printed Poly(lactic acid) with NaOH: A Systematic Approach. Polymers. 2020; 12(8);1711. doi.org/10.3390/polym12081711
15. Torre-Celeizabal A, Garea A, Casado-Coterillo C. Chitosan: Polyvinyl alcohol based mixed matrix sustainable coatings for reusing composite membranes in water treatment: Fouling characterization. Chemical Engineering Journal Advances. 2021;9:100236. doi.org/10.1016/j.ceja.2021.100236
16. Konegger T, Tsai CC, Bordia RK. Preparation of polymer-derived ceramic coatings by dip-coating. In Materials Science Forum (Vol. 825, pp. 645-652). Trans Tech Publications Ltd, 2015. doi.org/10.4028/www.scientific.net/MSF.825-826.645
17. Zarei M, Sayedain SS, Askarinya A, Sabbaghi M, Alizadeh R. Improving physio-mechanical and biological properties of 3D-printed PLA scaffolds via in-situ argon cold plasma treatment. Scientific Reports. 2023;13(1):14120. doi.org/10.1038/s41598-023-41226-x.
18. Kokubo T, Kushitani H, Sakka S, Kitsugi T, Yamamoto T. Solutions able to reproduce in vivo surface-structure changes in bioactive glass-ceramic A-W3. Journal of Biomedical Materials Research. 1990;24(6):721–734. doi.org/10.1002/jbm.820240607
19. Maçon ALB, Kim TB, Valliant EM, Goetschius KL, Brow RK, Day D.E, et al. A unified in vitro evaluation for apatite-forming ability of bioactive glasses and their variants. Journal of Materials Science: Materials in Medicine. 2015:26(2). doi.org/10.1007/s10856-015-5403-9
20. Ghorbani F, Li D, Ni S., Zhou Y, Yu B. 3D printing of acellular scaffolds for bone defect regeneration: A review. Materials Today Communications. 2020;22:100979. doi.org/10.1016/j.mtcomm.2020.100979
21. Seng CT, Noum SYAE, Sivanesan SKA, Yu L. Reduction of hygroscopicity of PLA filament for 3D printing by introducing nano silica as filler. AIP Conference Proceedings. 2020; 2233(1):020024. doi.org/10.1063/5.0001927
22. Saini P, Arora M, Kumar MR. Poly(lactic acid) blends in biomedical applications. Advanced Drug Delivery Reviews. 2016;107:47–59. doi.org/10.1016/j.addr.2016.06.014
23. Liu Y, Wang S, Zhang R, Lan W, Qin W. Development of Poly(lactic acid)/Chitosan Fibers Loaded with Essential Oil for Antimicrobial Applications. Nanomaterials. 2017;7(7):194. doi.org/10.3390/nano7070194
24. DeStefano V, Khan S, Tabada A. Applications of PLA in modern medicine. Engineered Regeneration. 2020;1:76–87. doi.org/10.1016/j.engreg.2020.08.002
25. Devarakonda S, Subramanian AK, Sivashanmugam P. Characterization of Polyvinyl Alcohol-Chitosan (PVA-CS) coating on Magnesium for Bio-Implant applications: A preliminary In Vitro study. World Journal of Dentistry. 2025;15(10),869–874. doi.org/10.5005/jp-journals-10015-2467
26. Tahir M, Vicini S, Jędrzejewski T, Wrotek S, Sionkowska A. New composite materials based on PVA, PVP, CS, and PDA. Polymers. 2024:16(23),3353. doi.org/10.3390/polym16233353
27. Oh S. Fabrication and characterization of hydrophilic poly(lactic-co-glycolic acid)/poly(vinyl alcohol) blend cell scaffolds by melt-molding particulate-leaching method. Biomaterials. 2016;24(22):4011–4021. doi.org/10.1016/s0142-9612(03)00284-9
28. Melčová V, Krobot , indelář J, ebová E, Rampichová MK, Přikryl R. The effect of surface roughness and wettability on the adhesion and proliferation of Saos-2 cells seeded on 3D printed poly(3-hydroxybutyrate)/polylactide (PHB/PLA) surfaces. Results in Surfaces and Interfaces. 2024;16;100271. doi.org/10.1016/j.rsurfi.2024.100271
29. Bahraminasab M, Doostmohammadi N, Talebi A, Arab S, Alizadeh A, Ghanbari A, et al. 3D printed polylactic acid/gelatin-nano-hydroxyapatite/platelet-rich plasma scaffold for critical-sized skull defect regeneration. Biomedical Engineering, 2022;21(86). doi.org/10.1186/s12938-022-01056-w

30. Chen S, Gil CJ, Ning L, Jin L, Perez L, Kabboul G, et al. Adhesive tissue Engineered scaffolds: Mechanisms and applications. Frontiers in Bioengineering and Biotechnology. 2021; 9: 683079. doi.org/10.3389/fbioe.2021.683079
31. Pei X, Wang J, Cong Y, Fu J. Recent progress in polymer hydrogel bioadhesives. Journal of Polymer Science. 2021;59(13),1312–1337. doi.org/10.1002/pol.20210249
32. Krishna PH, DhilipKumar T, Shankar KV, Hariprasad M, Murali AP, El-Rayyes A, et al. Review on Nature-Inspired interfaces and mechanical interlocking techniques in additively manufactured adhesively bonded joints. Journal of Materials Research and Technology. 2025;39:998-1016. doi.org/10.1016/j.jmrt.2025.09.150
33. Raynaud S, Champion E, Bernache-Assollant D, Thomas P. Calcium phosphate apatites with variable Ca/P atomic ratio I. Synthesis, characterisation and thermal stability of powders. Biomaterials. 2002;23(4),1065–1072. doi.org/10.1016/s0142-9612(01)00218-6
34. Eliaz N, Metoki N. Calcium phosphate Bioceramics: A review of their history, structure, properties, coating technologies and biomedical applications. Materials, 2017;10(4):334. doi.org/10.3390/ma10040334